

Article

On the Cold Deformation Behaviour of Two Phase TiAl Alloy with and without Void Defects

Firstname Lastname^{1,†,‡}, Firstname Lastname^{1,‡} and Firstname Lastname^{2,*}

¹ School of Mechanical and Electronical Engineering, Lanzhou University of Technology, Lanzhou 730050, China; e-mail@e-mail.com

² Affiliation 2; e-mail@e-mail.com

* Correspondence: e-mail@e-mail.com; Tel.: +x-xxx-xxx-xxxx

† Current address: Affiliation 3

‡ These authors contributed equally to this work.

Version October 2, 2018 submitted to Journal Not Specified

Abstract: Fracture processes of nanocrystalline metallic materia is affected by dislocation, nanovoid and other defects. Existing studies of defect evolution in titanium-aluminium alloy cover the case that voids located in single crystals, inside grain in poly crystals and at the grain boundaries. Molecular dynamics simulation was performed to study the evolution of a spherical nanovoid in $\alpha+\gamma$ two-phase titanium-aluminium alloy under uniaxial tension. The results show that voids located at the α/γ phase boundary have significant detract to strength of Ti-Al polycrystalline.

Keywords: $\alpha + \gamma$ two phase TiAl alloy; void; molecular dynamics

8

- 9 1. Vu, T.T.; Zehender, T.; Verheijen, M.A.; Plissard, S.R.; Immink, G.W.G.; Haverkort, J.E.M.; Bakkers, E.P.A.M. High optical quality single crystal phase wurtzite and zincblende InP nanowires. *Nanotechnology* **2013**, *24*, 115705. doi:10.1088/0957-4484/24/11/115705.
- 10 2. Kim, Y.W. Effects of microstructure on the deformation and fracture of γ -TiAl alloys. *Materials Science and*
- 11 *Engineering: A* **1995**, *192-193*, 519–533. doi:10.1016/0921-5093(94)03271-8.
- 12 3. Xiong, L.; Xu, S.; McDowell, D.L.; Chen, Y. Concurrent atomistic-continuum simulations of dislocation-void
- 13 interactions in fcc crystals. *International Journal of Plasticity* **2015**, *65*, 33–42. doi:10.1016/j.ijplas.2014.08.002.

16 1. Introduction

17 TiAl alloy has been used as structural material in aviation industry because its inherent advantages
18 such as low density and self-diffusion rates, high elastic module and high strength [1]. Two-phase
19 titanium aluminum alloys with proper phase distribution and grain size exhibit better mechanical
20 performance compared with monolithic constituents γ (TiAl) and γ (Ti₃Al) alloy [2]. Brittle fracture in
21 TiAl alloy strongly affects the safety of fracture of structure like turbo of aircraft engine and combustion
22 generator.

23 Deformation phenomena in TiAl alloys have been widely studied in order to overcome the
24 problems associated with the limited ductility and damage tolerance. The literature data covers a
25 wide range of parameters such as alloy composition, microstructure and deformation temperature.
26 Much of the work has been performed on single phase γ alloys and PST crystals. Rupture failure at
27 the macroscopic scale can be attributed to nucleation, growth and propagation of cracks, but at the
28 microscopic scale cracks are initially easily formed at defects in the casting process, such as voids
29 and inclusions [3]. These defects are known to play a fundamental role in the deformation of the
30 material. Nucleation, growth and coalescence of voids are deemed as the primary mechanism of

31 ductile material fracture, in which void growth is particularly important. Therefore, it is necessary to
 32 study the deformation response of porous materials with the consideration of microstructure evolution.

33 Brittle fracture in TiAl alloy strongly affects the safety of fracture of structure like turbo of aircraft
 34 engine and combustion generator [1]. Defects such as grain boundary, void and segregation plays an
 35 significant role in the process of fracture [2]. In order to understand the mechanism of brittle fracture,
 36 multi-scale methods from micro to macro scale have been applied to investigate the behavior of
 37 fracture. It's necessary to carefully examine the evolution of defects and its influence on the fracture
 38 process at atomic scale. A previous study on void growth in gamma-TiAl single crystal has revealed that
 39 void with high volume fraction detracts incipient yield strength [3]. Molecular dynamics (MD) method
 40 has been used to investigate the evolution of void in materials in nanoscale [4]. The fracture mechanisms
 41 in the duplex micro-structure are plasticity induced grain boundary decohesion and cleavage, while
 42 those in the lamellar microstructure are interface delamination and cracking across the lamellae [5].

43 MD simulations have revealed that existence of voids alone may contribute to strain hardening
 44 because they are barriers to dislocation movement [3].

45 2. Molecular Dynamics Simulation

46 2.1. Atomic Potential

47 The interaction of particles in the material is determined by interatomic potential. Many reported
 48 examples of crack propagation in metal materials were performed with embedded atom method
 49 due to its better accuracy in metal lattice compared with F-S and L-J [6]. The embedded atom method
 50 (MEAM) potential developed by Zope and Mishin [7] was used in the study. The simulation is
 51 submitted by MD simulations with the Large-scale Atomic/Molecular Massively Parallel Simulator
 52 (LAMMPS) open-source code [8]. We performed constant-pressure and constant-temperature (NPT)
 53 molecular dynamics simulation.

$$E_{total} = \sum F_i(\rho_{h,i}) + \frac{1}{2} \sum_i \sum_{j \neq i} \phi_{ij}(R_{ij}) \quad (1)$$

54 where E_{total} is the total energy of the system, $\rho_{h,i}$ is the host electron density at atom i due to the
 55 remaining atoms of the system, $F_i(\rho)$ is the energy for embedding atom i into the background electron
 56 density ρ , and $\phi_{ij}(R_{ij})$ is the core-core pair repulsion between atoms i and j separated by the distance
 57 R_{ij} . It can be noted that F_i only depends on the element of atom i and ϕ_{ij} only depends on the elements
 58 of atoms i and j . The electron density is, as stated above, approximated by the superposition of atomic
 59 densities, namely

60 2.2. Model Creation of Crystalline

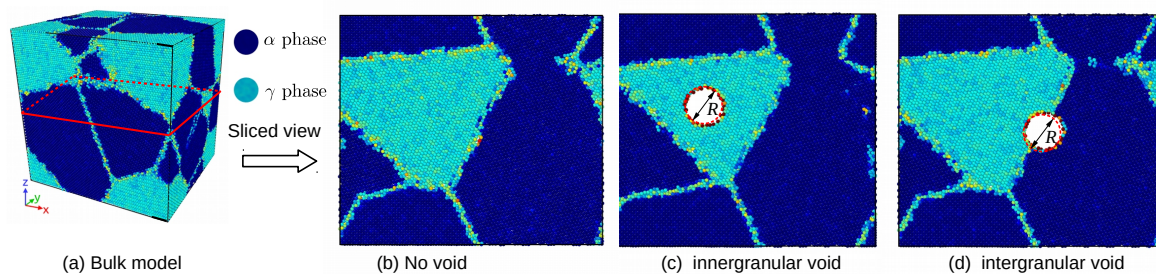


Figure 1. Overview of model creation

61 [9] γ TiAl has a fcc-centered tetragonal with an $L1_0$ structure [10], and α -TiAl is hcp structure, the
 62 structure of the two initial cells are shown in Fig. [11], and the constructing parameters are given by Table. [12].
 63 The simulation cells of two phase polycrystalline with an initially spherical void at different position

are shown in figure [1]. Periodic boundary conditions (PBC) are applied along all three directions, that makes poly crystal with periodic nanovoid structures. The initial dimension of simulation cell is $L_x = \text{nm}$, $L_y = \text{nm}$, $L_z = \text{nm}$, and each model contains about 4.6 million atoms. The grain orientation and size were randomly created with Voronoi method with code ATOMSK [1], and resulting in the arbitrary shape and orientation of the grains. Only one spherical void defect was placed intragranularly or intergranularly within each simulation model void within each simulation model. The intragranular spherical void was located in grain interior of the largest grain of the simulation model, as shown in Fig. [1]. The intergranular spherical void was at the center of the simulation cell, as shown in Fig. [1].

Table 1. Parameters of nanocrystalline

Phase	Space group	Designation	Parameters
α_2	P6 ₃ /mmc	O ₁₉	$a = 0.5765$ $c = 0.46833$
γ	tP4	L1 ₀	$a = 0.3997$ $c = 0.4062$

2.3. Analysis method

The centrosymmetry parameter is defined as follow:

$$P = \sum_{i=1}^6 |\vec{R}_i + \vec{R}_{i+6}|^2 \quad (2)$$

where \vec{R}_i and \vec{R}_{i+6} are the vectors corresponding to the six pairs of opposite nearest neighbors in the fcc lattice. The centrosymmetry parameter(CSP) is zero for atoms in a perfect lattice. In other words, if the lattice is distorted the value of P will not be zero. Instead, the parameter will have a value within the range corresponding to a particular defect. By removing all the perfect and surface atoms within the bulk, the existence of dislocation atoms become visible.

3. Results and Discussion

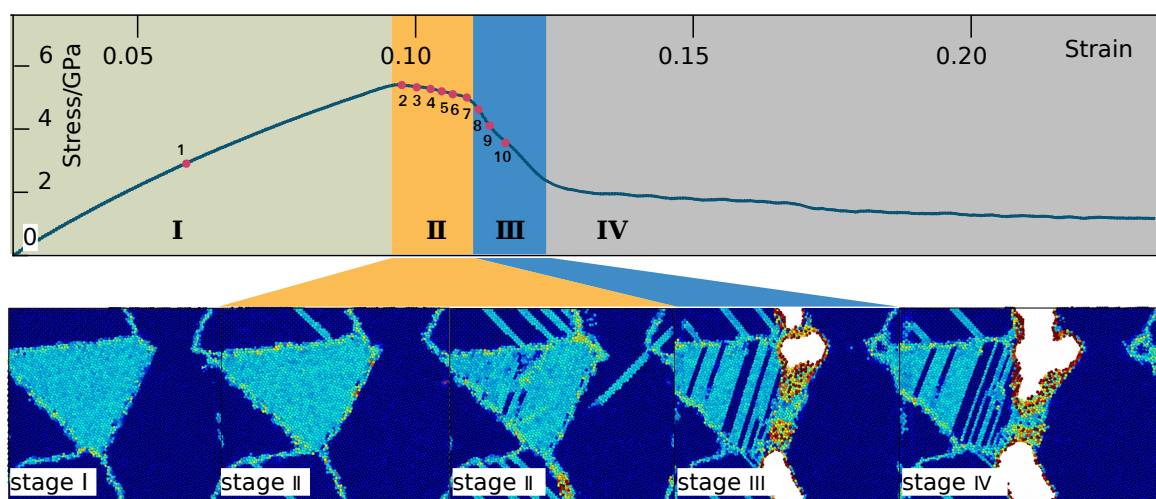


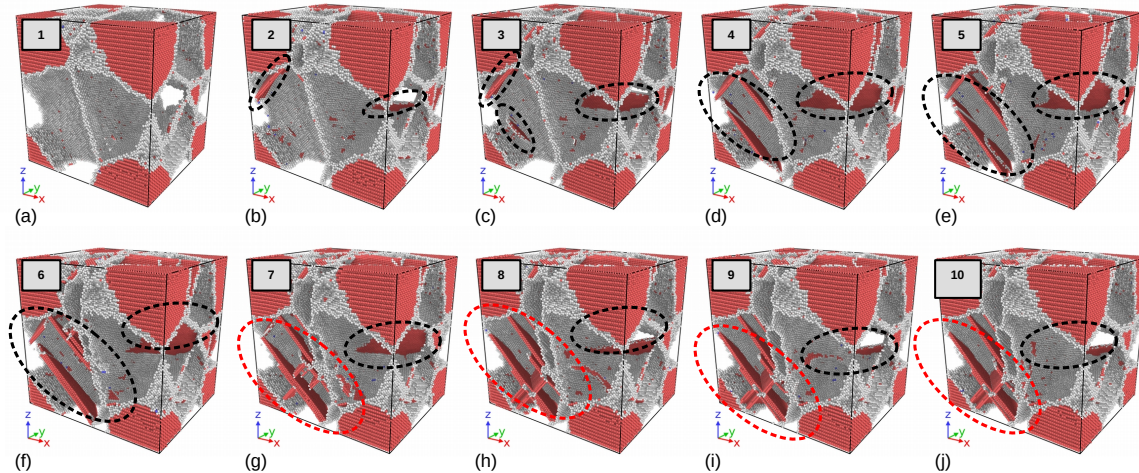
Figure 2. perfect-line2-2

Table 2. Key point during tensile process

Key Number	1	2	3	4	5	6	7	8	9	10
Time/ps	0	0.15	0.16	0.17	0.18	0.19	0.20	0.21	0.22	0.23
Strain	0	0.15	0.16	0.17	0.18	0.19	0.20	0.21	0.22	0.23

79 3.1. Deformation Behaviour of Two Phase Alloys without Void Defects

80 However, the following discussion concentrates on deformation phenomena that rely on the
 81 elastoplastic codeformation of the γ and γ_2 phases and on the particular point defect situation occurring
 82 in twophase alloys. Due to this effect ($\alpha_2 + \gamma$) alloys exhibit some remarkable properties that are
 unlike those of either constituent. The configure of atoms is shown in Fig.5, it can be seen that

**Figure 3.** γ phase deformation

83 dislocation emission initiate in γ pahse in XXX ps, and the deformation canbe mainly confied to the
 84 majority γ pahse. $\gamma(\text{TiAl})$ deforms by octahedral glide of ordinary dislocations with the Burgers
 85 vector $b=1/2<110]$ and superdislocations with the Burgers vectors $b=<101]$ and $b = 1/2 < 11\bar{2}]$. The
 86 other potential deformation mode is mechanical twinning along $1/6 < 11\bar{2}]111$. From Fig.5, of the
 87 two constituents of $(\alpha_2+\gamma)$ alloys, the α_2 phase is more difficult to deform. A reason for the unequal
 88 strain partitioning between the α_2 and γ phase is certainly the strong plastic anisotropy of the α_2
 89 phase. TEM examinations performed on tensile tested lamellar alloys have revealed that the limited
 90 plasticity of the α_2 phase is mainly carried by local slip of $<\text{a}>$ -type dislocations with the Burgers vector
 91 $b = 1/3 < 11\bar{2}0 >$ prism planes⁵, which is by far the easiest slip system in α_2 single crystals. Basic
 92 deformationg mechanism of α phase

93 1.In many cases the orientation of slip slip is changed because the crystallographically available
 94 slip and directions are not continuous across the interface. This may significantly reduce the Schmid
 95 factor and thus impede slip transfer. At the γ/γ interfaces the orientation of the slip plan could change
 96 through a relevantly large angle of about 90 degree. Reorientation of slip is always required at the
 97 α_2/γ interface; the smallest angle between the corresponding slip planes 111_γ and $10 - 10_{\alpha_2}$ is about
 98 19 degree [].

99 The core of a dislocation intersecting an interface often needs to be transformed. For example, an
 100 ordinary $1/2<110]$ dislocation gliding in one γ grain has to be converted in to a $<101]$ super dislocation
 101 with the double Burgers vector gliding in an adjacent γ grain. At the α/γ interface the dislocations
 102 existing in the $D0_{19}$ structure have to be transformed into dislocations consistent with the $L1_0$ structure.
 103 These core transformations are associated with a change of the dislocation line energy because the
 104 lengths of the Burgers vectors and the shear module are different.

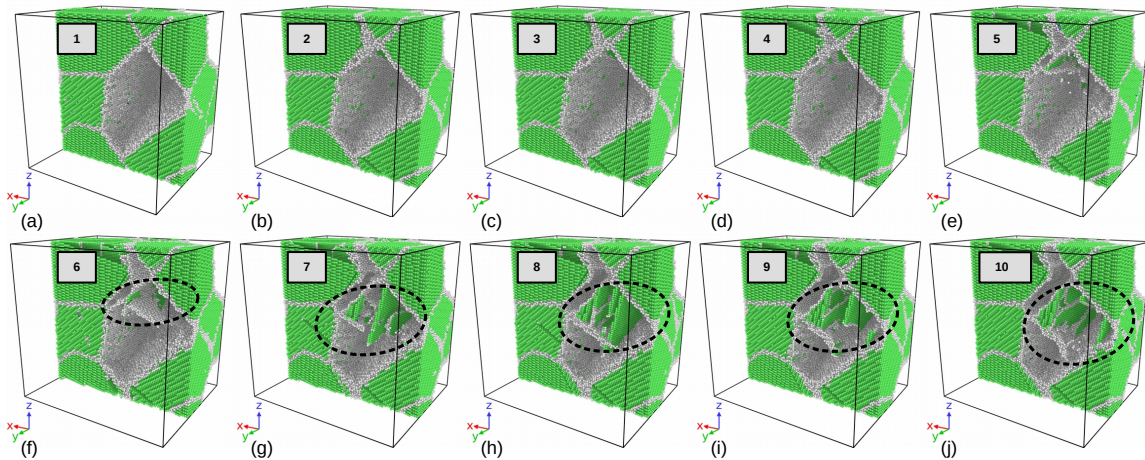


Figure 4. α phase deformation

106 Dislocations crossing semi-coherent boundaries have to intersect the misfit dislocations, a process
 107 that involves elastic interaction, jog formation and the incorporation of gliding dislocations into the
 108 mismatch structure of the interface. When the slip is forced to cross α_2 lamella, pyramidal slip of the α_2
 109 phase is required, which needs an extremely high shear stress.

110 *3.2. Evolution of spherical void in the simulation with intragranular spherical voids*

111 A step, of the width of a burgers vector, will be generated at both sidesof a crystal along teh
 112 direction of teh burgers vector after dislocation traversing teh entire crystal, as is shown in ???. A small
 113 step will be formed at spherical void surface toward teh void interiorafter dislocation absorptioanat
 114 sphericalvoid surfaces, as is shown in ???. If a great number of dislocation slip along their respective
 115 systemstowards teh spherical nanovoid in all directions, and are absorbed at spherical void surfaces,
 116 the spherical nanovoid will eventually shrink from teh dash circle to

117 *3.3. The effect of void on the strength of material*

118 Void of R=10 was placed at phase boundary, inside α phase grain respectively. Effect of void at
 119 different position under uniaxial tension is shown in Fig.10. The strength of materails with void in
 120 different size and at different position is shown in Fig.10. The results show that the model without
 121 void defect has best stength, while the void loacted inside α phase detracts the strength of the material
 122 most, and the void at the phase boundary have less impact on the strength.

123 The effect of siz is expectable that the greater voids detracts the strength of the materials more,
 124 however, it has been observed in the simulation that there is a critical value about 15A for voids at
 125 different position. The voids larger than 15 A have dramatic detraction to the strength of the material.
 126 Conventional definition of strength of materails with geometry subtraction was applied to the model,
 127 and theroticial strength of the models was calculated by formulation 3:

$$\sigma^* = \sigma_0 \cdot \frac{A^*}{A_0} \quad (3)$$

128 where σ_0 is the strength of the model without void defects 5.26 Gpa, and A_0 is initial section area,
 129 $A = a \times b = 36000A^2$, A^* is section area in consider of the subsection that results from the voids.
 130 Comparing with the strength determined by molecular dynamics simulation and the results calculated
 131 with formulation 3, it can be assumed that the main factor that affects the strength of materials can be
 132 attributed to local behaciour of the materials, thus revolution of defects should be examined carefully.

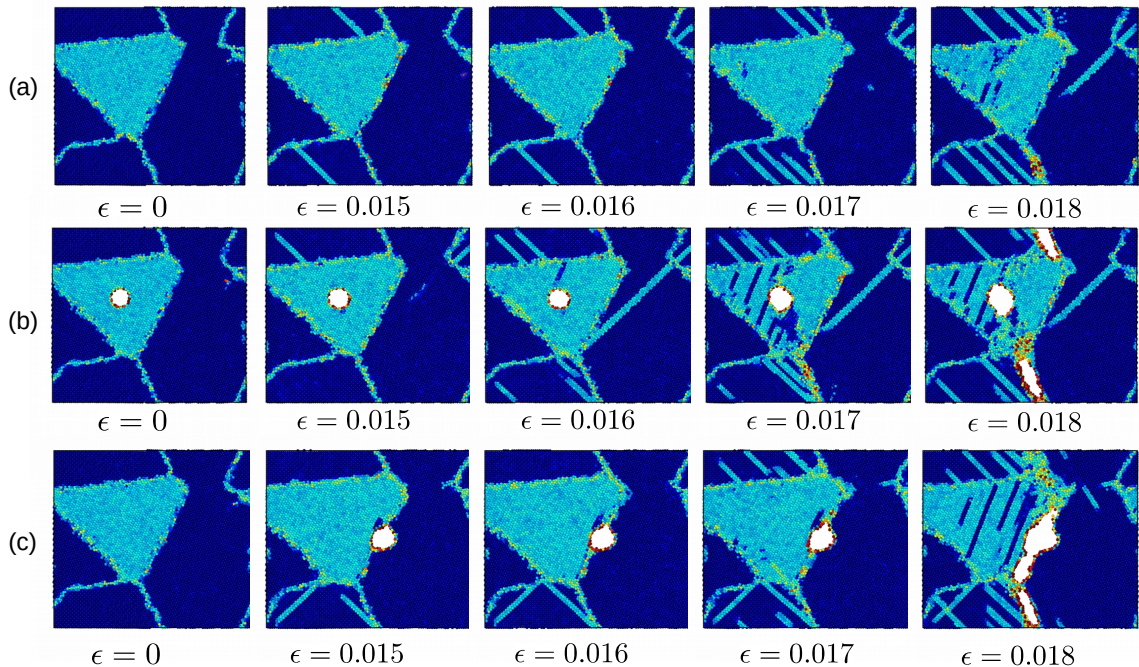


Figure 5. Yield process of the models

Voids with different size: 2A, 5A, 10A, 15A were placed into the model respectively. It has been observed that voids detracts the strengths of the material. The max stress stress of the simulation cell decreases as the volume of voids are lareger. From Fig ??, there is a critical value of void radius about 15A, the void greater than 15A cause serious detraction of strength of material. Engineering stress is calculated

$$\sigma = S/A$$

133 The rate of decrease of loading area are smaller comparing with the detraction of strength, so it can
 134 be assumed that the yield yield behaviour and strength is much more related with local behaviour of
 135 grain boundaries and void.

136 Grain and phase boundaris are obstancles to deformation process, thus the stability of boundaries
 137 have great impact on the strength of materials. Interactive between grainboundary and void determines
 138 the fracture mode of the TiAl alloy.

According to Schmid's law:

$$\tau = \sigma * m$$

where m is the Schmid factor :

$$m = \cos(\phi)\cos(\lambda)$$

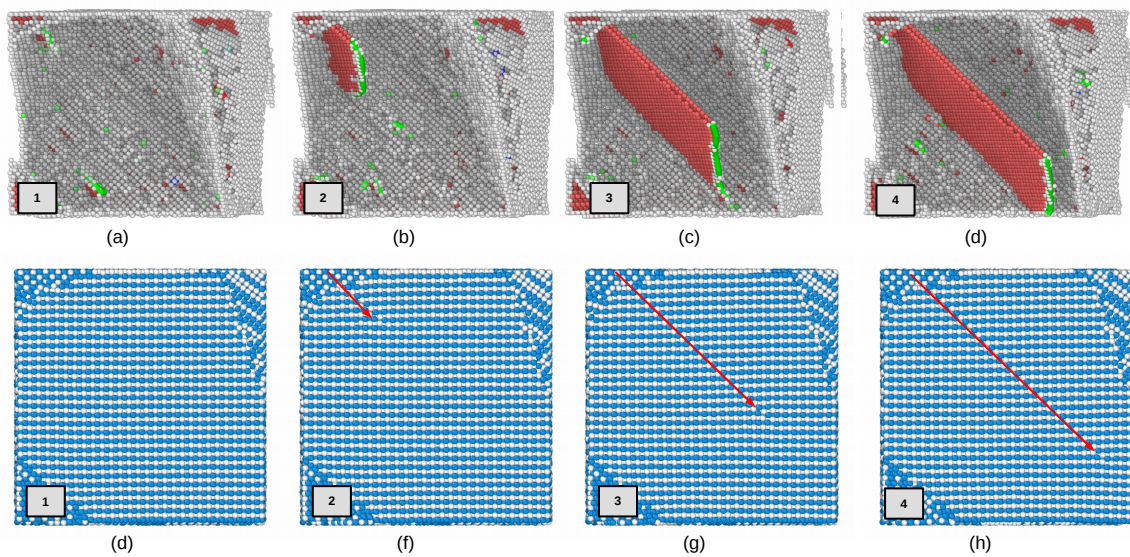


Figure 6. Dislocation in γ

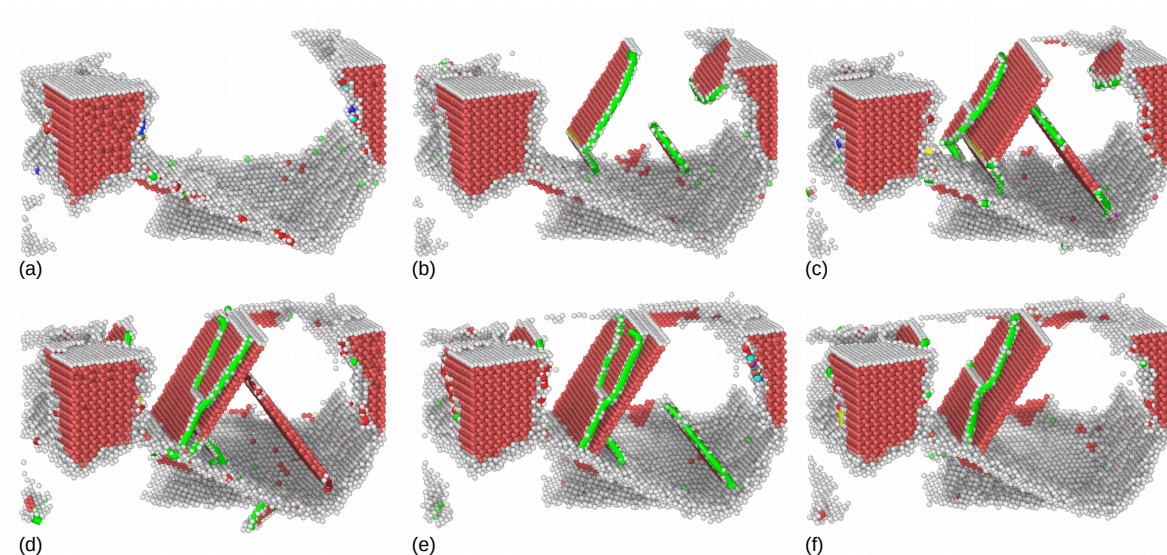
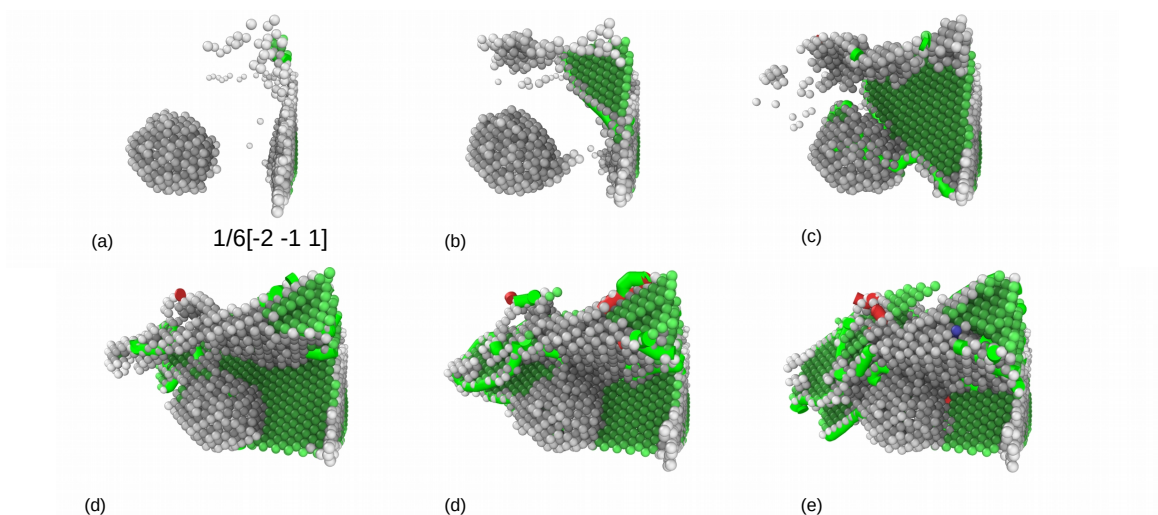
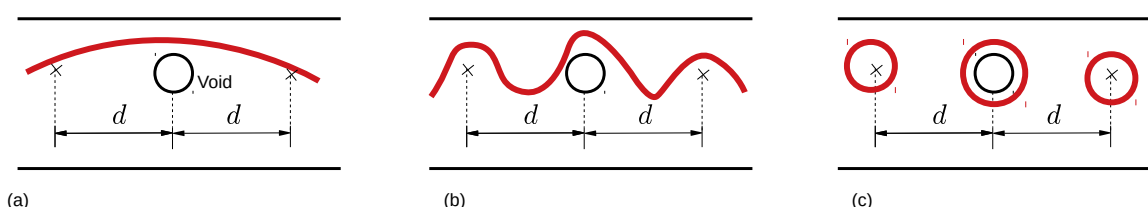
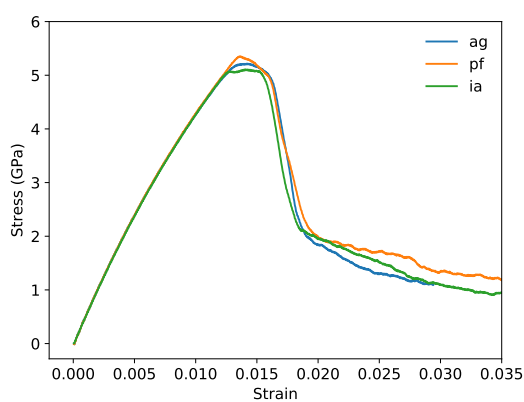
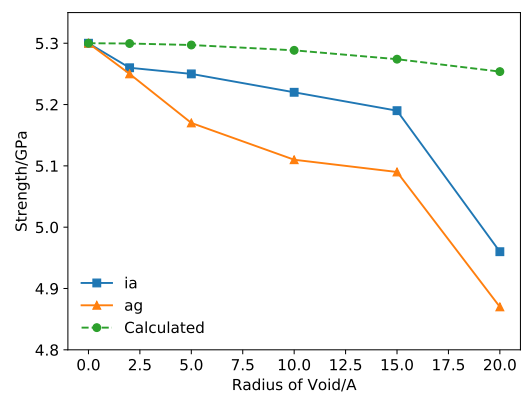


Figure 7. stress-strain curve

**Figure 8.** Dislocation around void**Figure 9.** orowan**Figure 10.** Stress-Strain**Figure 11.** Strength of models